

# Constraints on low-x PDFs from Drell Yan processes, and first studies of exclusive dimuon production with the LHCb experiment

Jonathan Anderson for the LHCb Collaboration

Physik-Institut der Universität Zürich, Winterthurerstrasse 190, 8057 Zürich, Switzerland

DOI: <http://dx.doi.org/10.5689/UA-PROC-2010-09/28>

We summarise the results from early LHCb data for muon final states produced through the Drell-Yan process via W, Z and  $\gamma^*$  down to a  $Q^2$  of  $5 \text{ GeV}^2$ . Extrapolating these results up to the sample sizes expected in the remainder of the 2010 run gives exciting prospects for parton density function studies, which will benefit from LHCb's unique ability to trigger on low transverse momentum objects. Due to the forward acceptance of LHCb, x values down to  $2 \times 10^{-6}$  can be probed, where with just  $100 \text{ pb}^{-1}$  of data the uncertainty on the gluon PDF can be reduced by more than a factor of two. We also report on first studies of exclusive  $\chi_c \rightarrow J\psi(\mu\mu)\gamma$  production at LHCb, an important calibration channel for exclusive Higgs production at the LHC.

## 1 Introduction

LHCb [1], one of the four large experiments at the Large Hadron Collider (LHC), has been primarily designed and built to make measurements of CP-violating and rare decays in the b-quark sector. Due to the  $b\bar{b}$  production topology at the LHC, whereby both B hadrons are mostly produced in the same forward or backward cone, LHCb has been constructed as a forward single-arm spectrometer with an approximate coverage in terms of pseudorapidity of  $1.9 < \eta < 4.9$ . While a portion of this pseudorapidity range ( $1.9 < \eta < 2.5$ ) is also covered by the general purpose detectors ATLAS and CMS, the very forward region ( $\eta > 2.5$ ) is unique to LHCb. Due to its forward geometry, LHCb is capable of triggering on low transverse momentum ( $P_T$ ) objects. In addition to its main B physics programme, LHCb is capable of making precision electroweak measurements at high rapidities testing theoretical predictions and enabling the exploration of a large, previously unmeasured, kinematic region.

LHCb is now fully installed, commissioned and taking data. At the time of the ISMD2010 conference in the middle of September 2010, data corresponding to an integrated luminosity of  $3.5 \text{ pb}^{-1}$  had been collected. By the end of the 2010 proton-proton run this had increased to  $\sim 37 \text{ pb}^{-1}$ . In this contribution we present the first measurements of electroweak boson and exclusive  $\chi_c$  production at LHCb. In the 2011 run it is hoped to accumulate  $\sim 1 \text{ fb}^{-1}$  of data. In this report we consider the potential improvements to the proton PDFs that could be achieved with a smaller dataset of  $100 \text{ pb}^{-1}$ .

## 2 Electroweak boson production at LHCb

Figure 1(a) shows the kinematic regions probed by events at LHCb in terms of the longitudinal fraction of the incoming proton's momentum carried by the interacting parton,  $x$ , and the square of the four-momentum exchanged in the hard scatter,  $Q^2$ . For particle production processes at LHCb, the momenta of the two interacting partons will be highly asymmetric, meaning that events at LHCb will simultaneously probe a region at high- $x$  and a currently unexplored region at very low- $x$ . The Drell-Yan processes  $\gamma^*/Z \rightarrow \mu\mu$  and  $W \rightarrow \mu\nu$ , having simple and distinctive final states, provide an ideal laboratory for investigating this unexplored region. The main theoretical uncertainties on cross-section predictions for electroweak boson production at the LHC stem from the level of knowledge of the input proton PDFs. From the point of view of LHCb, PDFs have been determined from fixed target data and to a lesser extent HERA data for the larger  $x$  values and confirmed at higher  $Q^2$  by  $W$  and  $Z$  production at the Tevatron. For the smaller  $x$  values, the PDFs have been measured by HERA alone but at much lower  $Q^2$  from where they must be evolved to higher energies using the DGLAP equations.

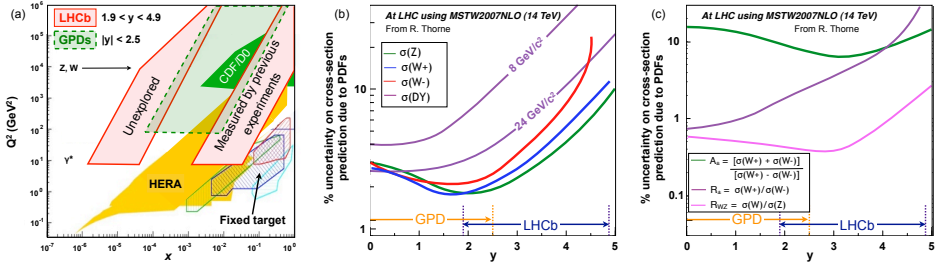


Figure 1: (a) The kinematic range in  $x - Q^2$  space probed at LHCb and the general purpose LHC detectors (GPDs). The regions covered by measurements at previous experiments are shown. (b) Percentage uncertainty on cross-section predictions for  $W$ ,  $Z$  and low mass Drell-Yan pairs at the LHC due to the PDFs as a function of rapidity. The regions fully instrumented by LHCb and the GPDs are shown (from [2]). (c) Percentage uncertainty on predictions for the ratio and asymmetry of  $W$  and  $Z$  production at the LHC due to the PDFs. (from [2]).

Measurements of the differential cross-sections for electroweak bosons decaying to muon final states at LHCb and the ratios of these cross-sections can provide useful information on both the PDFs and QCD. Figure 1(b) shows the percentage uncertainty on cross-section predictions for  $W$ ,  $Z$  and  $\gamma^*$  production at the LHC due to the uncertainty on the PDFs. While the expected uncertainty on  $W$  and  $Z$  production is expected to be small, meaning that a measurement of these cross-sections will constitute either a good test of QCD or enable a precision luminosity determination, the expected uncertainty on  $\gamma^*$  production gets larger for smaller boson masses and higher boson rapidities [2]. Therefore, by measuring the differential cross-section for the  $\gamma^* \rightarrow \mu\mu$  process for a variety of different invariant masses, sections of  $x$ - $Q^2$  space can be mapped out yielding large improvements to the PDFs. LHCb has a particular advantage over ATLAS and CMS in accessing the least understood regions due to its higher rapidity range and lower muon transverse momentum trigger thresholds which will allow exploration down to  $Q^2=6.25$  GeV<sup>2</sup>/c<sup>4</sup>. LHCb will therefore have the unique ability to measure PDFs down to  $x \approx 10^{-6}$ , below the smallest values accessible at HERA and explore a totally unknown, and important, kinematic domain. In addition, as shown in Figure 1(c) a measurement of both

the ratio and asymmetry of  $W^+$  to  $W^-$  production can provide valuable constraints on the PDFs while a measurement of the ratio of  $W$  to  $Z$  production, being almost unaffected by PDF uncertainties, will provide a precision test of the Standard Model.

### 3 Electroweak boson candidates with early LHCb data

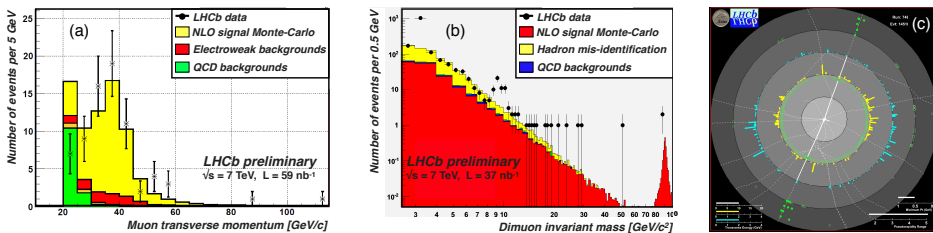


Figure 2: (a) Transverse momentum distribution of muons passing the offline  $W$  selection. Expected signal and background distributions are also shown. (b) Dimuon invariant mass distribution for events passing the offline  $\gamma^*/Z \rightarrow \mu\mu$  selection. Expected signal and background distributions are also shown. (c) Example of a candidate  $Z \rightarrow \mu\mu$  event at LHCb shown in a  $\phi - z$  projection. The solid lines denote reconstructed tracks whose length represents the track  $P_T$ . Muon station hits are shown in green.

A search for  $W \rightarrow \mu\nu$  and  $\gamma^*/Z \rightarrow \mu\mu$  candidate events has been performed using the first  $\sim 50 \text{ nb}^{-1}$  of LHCb data. Since disagreements between data and simulation are to be expected, the data themselves have been used as much as possible to understand the backgrounds. In order to remove ghost tracks and reduce a variety of QCD and electroweak backgrounds, only muon tracks with a probability  $\chi^2$  greater than 0.001, a relative momentum uncertainty less than 10%, an impact parameter that is compatible with the primary vertex and that have at least 5 associated hits in the muon stations are considered.

The signature for a  $W \rightarrow \mu\nu$  decay consists of a single high  $P_T$  isolated muon and little other activity in the event. In order to isolate  $W$  candidate events, this distinctive topology is exploited by requiring that the asymmetry of the muon  $P_T$  and the vector sum of the transverse momenta of all of the other tracks in the event ( $A_{P_T}$ ) is greater than 0.65. For events satisfying this requirement, figure 2(a) shows a comparison between the muon  $P_T$  distribution measured with the first  $59 \text{ nb}^{-1}$  of LHCb data and the next to leading order (NLO) prediction obtained using the MCFM Monte-Carlo generator [3]. The dominant QCD background is due to hadrons that have been mis-identified as muons. This background has been determined from data by examining the fraction of tracks in a large minimum bias sample that are mis-identified as muons. The electroweak backgrounds have been determined from Monte-Carlo. Here the dominant contribution is due to  $Z \rightarrow \mu\mu$  decays where only one of the muons is produced inside the LHCb acceptance. In total 66  $W$  candidates have been found in agreement with the NLO Monte-Carlo expectation.

$\gamma^*/Z \rightarrow \mu\mu$  events have been selected by requiring two muons that have momenta greater than 10 GeV/c and impact parameters that are compatible with the primary vertex. Figure 2(b) shows the resulting dimuon invariant mass distribution using the first  $37 \text{ nb}^{-1}$  of LHCb data. Again the backgrounds due to hadron mis-identification have been determined from data

while the other QCD backgrounds, primarily due to heavy quark decays, have been estimated using Monte-Carlo. The backgrounds from other electroweak processes have not been included but are expected to be at a level of less than 1% of the signal level [4]. At the Z mass, where purities of  $\sim 99\%$  are expected, two candidate  $Z \rightarrow \mu\mu$  decays are observed in agreement with NLO Monte-Carlo expectations. Figure 2(c) shows a graphical representation of one of these Z candidates in a  $\phi - z$  view of the LHCb detector. Here the solid lines represent reconstructed tracks where the length of the line denotes the track  $P_T$  while the green points represent the muon station hits that have been associated to the tracks. It can be seen that aside from the two high  $P_T$  muon tracks the event contains little other activity. In the low mass region the backgrounds have been found to be lower than expected from Monte-Carlo simulations. While work is ongoing to understand this discrepancy, the prospects for isolating high purity samples in this region are positive [4].

With  $37 \text{ pb}^{-1}$  of data now on tape, full W, Z and  $\gamma^*$  cross-section measurements are expected in the near future.

## 4 Potential PDF constraints with early LHCb data

The expected improvement to the proton PDFs when including W, Z and  $\gamma^*$  cross-section measurements from LHCb has been investigated using  $100 \text{ pb}^{-1}$  of dummy LHCb data. We have considered the effect on the following sets, MSTW08[5], CTEQ66[6], Alekhin[7] and NNPDF2.0[8]. A more detailed description of the method can be found in [9].

For the PDF sets obtained by performing a global fit based on a Hessian method (MSTW08, CTEQ66 and Alekhin), the improvement has been assessed in the following way. A given physical observable,  $f$ , can be described as a linear combination of the observable obtained using the PDF best-fit,  $f_0$ , and the observable  $f_i$  obtained by moving the  $i$ th eigenvector by 1-sigma.

$$f = f_0 + \Sigma[f_0 - f_i]\lambda_i \quad (1)$$

The one sigma bound is mapped out by sampling  $\lambda_i$  from a unit Gaussian with mean zero; this function also provides a form with which the data can be fitted. Given binned data with  $N_j$  events in the  $j$ th bin with error  $\delta_j$ , the normalization and the shape of the distribution can be fitted by minimizing

$$\chi^2 = \Sigma \left[ \frac{N_j - \lambda_0(f_0 + \Sigma\lambda_i(f_0 - f_i))}{\delta_j} \right]^2 + \Sigma\lambda_i^2 \quad (2)$$

where  $\lambda_0$  is the overall luminosity and  $\lambda_i$  are the fitted eigenvalues. Before the fit the eigenvalues of the model by definition have an uncertainty equal to 1. After our fit, values smaller than 1 imply that we have a better constraint on the PDF.

In the case of NNPDF2.0, a PDF set produced using a neural network approach based on Monte-Carlo replicas, the expected improvement is determined by comparing the dummy LHCb data to a large number of replicas. The compatibility of the dummy data to each replica is evaluated as a  $\chi^2$  probability. It is then possible to constrain the PDFs considering the  $\chi^2$  probability as the conditional probability for measuring the set of NNPDF replicas considering the new LHCb data.

It is expected that the combined effect of  $100 \text{ pb}^{-1}$  of LHCb W and Z data will be to reduce the uncertainty on the  $u_v$ ,  $d_v$ ,  $s^+$ , sea and gluon distributions by  $\sim 10\%$ . Figure 3 shows the

ratio between the uncertainty on the distributions before and after the inclusion of  $100 \text{ pb}^{-1}$  of dummy LHCb  $\gamma^*$  ( $10 \text{ GeV}/c^2 < M_{\mu\mu} < 20 \text{ GeV}/c^2$ ) data. Here the improvements are expected to be more dramatic, particularly for the gluon and sea quark distributions at low- $x$  where a  $\sim 50\%$  reduction in uncertainties is expected.

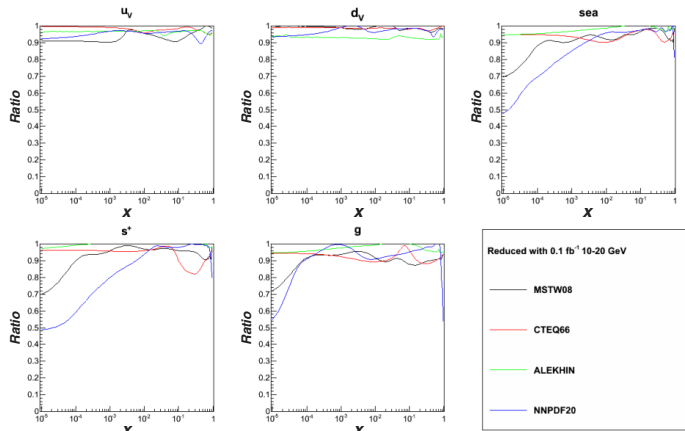


Figure 3: Ratio between PDF uncertainties before and after adding  $100 \text{ pb}^{-1}$  of  $\gamma^* \rightarrow \mu\mu$  ( $10 \text{ GeV}/c^2 < M_{\mu\mu} < 20 \text{ GeV}/c^2$ ) LHCb data for different distributions as a function of  $x$ .

## 5 Exclusive $\chi_c$ production at LHCb

Since they provide a clean environment in which to measure the quantum numbers of new states, measurements of exclusive production processes in high energy proton-proton collisions represent a promising laboratory for studying a variety of new particles, most notably the exclusive production of Higgs bosons. Measurements of the exclusive production of  $\chi_c$  mesons, being driven by the same production mechanism as exclusive Higgs production but having a much higher cross-section, will constitute a valuable cross-check of theoretical predictions for exclusive production processes.

Exclusive  $\chi_c \rightarrow J/\psi(\mu\mu)\gamma$  events have been isolated in the first  $1 \text{ pb}^{-1}$  of LHCb data by requiring a reconstructed dimuon pair, photon and no other activity in the event. Figure 4(a) shows the resulting dimuon-photon invariant mass distribution. Four candidate events have been found with masses compatible with the  $\chi_c$  mass, in agreement with expectations from the SuperChiC Monte-Carlo generator [10]. Figure 4(b) shows a graphical representation of one of these candidates in a  $\phi - z$  view of the LHCb detector.

## 6 Conclusions

Due to the fact that it is fully instrumented in the forward region and has low muon transverse momentum trigger thresholds, events at LHCb will explore a unique region in  $x - Q^2$  space. The Drell-Yan processes  $\gamma^*/Z \rightarrow \mu\mu$  and  $W \rightarrow \mu\nu$ , having simple and distinctive final states, provide an ideal laboratory for exploring this currently unmeasured region. Using the first data

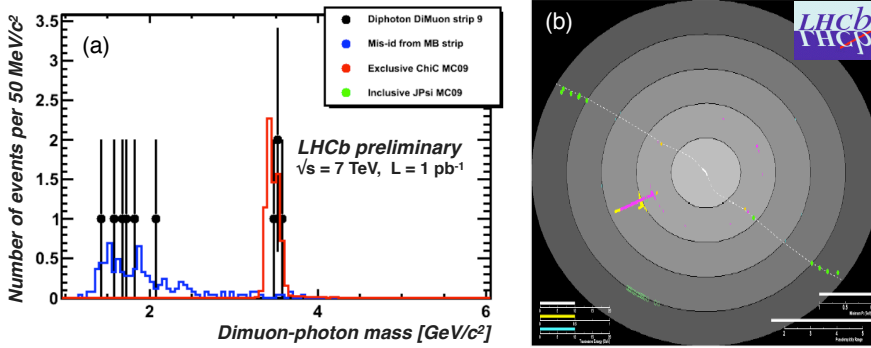


Figure 4: (a) Dimuon-photon invariant mass distribution for exclusive  $\mu\mu\gamma$  events at LHCb. The expected contribution from to exclusive  $\chi_c$  events, predicted by the SuperChiC Monte-Carlo generator, is shown in red. (b) Example of a candidate exclusive  $\chi_c$  event at LHCb shown in a  $\phi - z$  projection. The solid lines denote reconstructed tracks whose length represents the track  $P_T$ , muon station hits are shown in green while calorimeter clusters are shown in purple.

from LHCb, candidate W and Z events have been isolated. With  $37 \text{ pb}^{-1}$  of data now on tape, it is expected that full cross-section measurements will be made in the coming months. These measurements will provide valuable tests of QCD and place constraints on the proton PDFs. With as little as  $100 \text{ pb}^{-1}$  of data a reduction of up to 50% is expected to the uncertainty on the gluon and sea quark distributions at low x. Finally, we have presented the first exclusive  $\chi_c$  candidate events found at LHCb. When more data are analysed, these events will place valuable constraints on theoretical predictions of exclusive particle production processes at the LHC.

## References

- [1] The LHCb collaboration, *The LHCb Detector at the LHC*, JINST **3** S08005 (2008).
- [2] R. Thorne, *Parton Distributions and QCD at LHCb*, DIS2008 London, arXiv:0808.1847v1 [hep-ph] (2008).
- [3] J. M. Campbell and R. K. Ellis, *A Monte Carlo for FeMtobarn processes at Hadron Colliders*, <http://mcfm.fnal.gov/mcfm.pdf>
- [4] J. Anderson, *Probing low-x with Drell-Yan events at LHCb*, XVII International Workshop on Deep-Inelastic Scattering and Related Subjects, Madrid, Spain, Apr 2009, LHCb-PROC-2009-014 (2009).
- [5] A.D. Martin, W.J. Stirling, R.S. Thorne, G. Watt, "Parton distributions for the LHC", arXiv:hep-ex/0901.0002v2 (2009).
- [6] J. Pumplin, D.R. Stump, J. Huston, H.L. Lai, P. Nadolsky, W.K. Tung, "New Generation of Parton Distributions with Uncertainties from Global QCD Analysis", JHEP0207:012 (2002).
- [7] S. I. Alekhin, Phys. Rev. D **63**, 094022 (2001).
- [8] R. D. Ball, L. Del Debbio, S. Forte, A. Guffanti, J. I. Latorre, A. Piccione, J. Rojo, M. Ubiali, *A first unbiased global NLO determination of parton distributions and their uncertainties*, arxiv:hep-ph:1002.4407 (2010).
- [9] F. De Lorenzi, *PDF sensitivity studies at LHCb*, XVIII International Workshop on Deep-Inelastic Scattering and Related Subjects, Florence, Italy, Apr 2010, arxiv4.library.cornell.edu/pdf/1011.4260v1 (2010).
- [10] L.A. Harland-Lang, V.A. Khoze, M.G. Ryskin, W.J. Stirling, *Central exclusive  $\chi_c$  meson production at the Tevatron revisited*, arXiv:0909.4748 [hep-ph] (2009).